IP2016 / 4th International Workshop on Induced Polarization

3D TEM-IP inversion workflow for galvanic source TEM data

Seogi Kang
University of British Columbia
6339 Stores Rd., Vancouver, Canada
skang@eos.ubc.ca

Douglas W. Oldenburg
University of British Columbia
6339 Stores Rd., Vancouver, Canada
doug@eos.ubc.ca

SUMMARY

Electrical induced polarization (EIP) surveys have been used to detect chargeable materials in the earth. For interpretation of the time domain EIP data, the DC-IP inversion method, which first invert DC data (on-time) to recover conductivity, then inverts IP data (off-time) to recover chargeability, has been successfully used especially for mining applications finding porphyry deposits. It is assumed that the off-time data are free of EM induction effects. When this is not the case, an EM-decoupling technique, which removes EM induction in the observation, needs to be implemented. Usually responses from a half-space or a layered earth are subtracted. Recent capability in 3D TEM forward modelling and inversion allows us to revisit this procedure. Here we apply a 3D TEM-IP inversion workflow to the galvanic source example. This includes three steps: a) invert DC and early time channel TEM data to recover the 3D conductivity, b) use that conductivity to compute the TEM response at later time channels. Subtract this fundamental response from the observations to generate the IP response, and c) invert the IP responses to recover a 3D chargeability. This workflow effectively removes EM induction effects in the observations and produces better chargeability and conductivity models compared to conventional approaches.

Key words: Induced polarization, EM-decoupling, galvanic source, time domain EM, 3D inversion

INTRODUCTION

The electrical conductivity of earth materials can be frequency dependent with the effective conductivity decreasing with decreasing frequency due to the buildup of electric charges that occur under the applied electric field. Effectively, the rock is electrically chargeable. Controlled-source electromagnetic (EM) methods excite the earth using either galvanic (a generator attached to two grounded electrodes) or inductive source (arising from currents flowing in a wire loop). A typical EIP survey layout (Siegel, 1959) is shown in Figure 1.

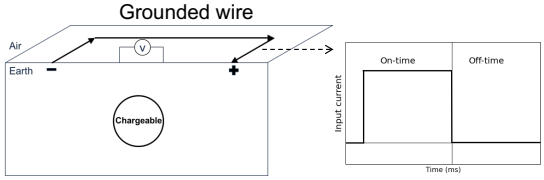

Figure 1. Conceptual diagram of a ground-based galvanic source with half-duty cycle current waveform.

It consists of grounded electrodes carrying a current waveform (like the square wave shown) and electrodes to measure voltage differences. When the ground is chargeable the received voltage looks like that in Figure 2. The decay in the off-time is the IP effect. To interpret observed IP data, a two-stage inversion is usually deployed (Oldenburg and Li, 1994). The first step is to invert late on-time data (V_0) using a DC inversion to obtain the background conductivity. The second step is to use the obtained conductivity to generate a sensitivity function, and then invert late off-time data (V_s); this is often called DC-IP inversion.

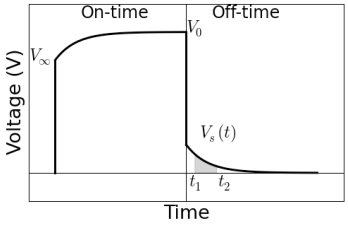

Figure 2. A typical overvoltage effects in EIP data.

Although application of this method has been successful, a main concern is the second step. The time decaying fields are assumed to be purely the result of IP phenomena and any EM induction effects in the data are ignored. This assumption can be violated when the earth has a significant conductivity and EM coupling can remain even in the late off-time. Removing the effects of EM induction from the measured data is referred to as EM-decoupling and it has been a focus of attention for many years. Most analyses have used simple earth structures: half-space and layered earth to ameliorate its effects (Wynn and Zonge, 1975). However, with our current capability to handle 3D forward modelling and inversion it is timely to revisit this issue.

In a recent work (Kang and Oldenburg, 2016), we developed a workflow for inverting airborne IP data using inductive sources. This involved three main steps: a) inverting early time TEM data to recover a 3D conductivity, b) EM-decoupling (forward modelling the EM response and then subtracting it from the observations), and c) IP inversion to recover pseudo-chargeability distribution at each time channel. The current problem of inverting IP data using grounded sources follows the same workflow but some aspects are greatly simplified because EIP measures data when electric fields, and charge accumulations, have reached a steady state. This provides another data set from which information about the electrical conductivity can be extracted.

A major difference between conventional EIP inversion and our approach is the use made of early time channels in the EIP data. In conventional work these have been considered as "noise" and hence been thrown away. However, we consider these as "signal" to recover conductivity. In this study, we apply a 3D TEM-IP inversion workflow to the synthetic galvanic source example (gradient array). This will include the three steps in the workflow listed above but the first step is altered so that we invert the DC data, and early time channels of TEM data, to recover the 3D conductivity.

SEPARATION OF EM AND IP RESPONSE

Assuming the earth has chargeable material, the observed responses from any TEM survey has both EM and IP

responses. To be more specific, we first define the complex conductivity in the frequency domain as

$$\sigma(\omega) = \sigma_\infty + \triangle\sigma(\omega) \quad (1)$$

where σ_∞ is the conductivity at infinite frequency, and ω is angular frequency (rad/s). For the Cole-Cole model from Pelton et al. (1978),

$$\triangle\sigma(\omega) = -\sigma_\infty \frac{\eta}{1+(1-\eta)(i\omega\tau)^c}, \quad (2)$$

where η is intrinsic chargeability, τ is time constant, and c is frequency dependency. Following Smith et al. (1988), the observed datum including both EM and IP effects can be defined as

$$d^{obs} = d^F + d^{IP}, \quad (3)$$

where d^F and d^{IP} are respectively the fundamental and IP responses. Here the fundamental response is $d^F \equiv F[\sigma_\infty]$, where F[·] is a Maxwell's operator; this takes the conductivity and computes EM responses without IP effects. Note that $\sigma(\omega) = \sigma_\infty$ when η=0. A main goal of our 3D TEM-IP inversion workflow is to evaluate the d^F and d^{IP} components. To illustrate the challenge, we perform a simple TEM forward modelling using a galvanic source as shown in Figure 1. We inject a half-duty cycle rectangular current through a grounded wire. A chargeable body is embedded in the earth. Figure 3 shows the measured voltage at a pair of potential electrodes on the surface. It is different from the conventional over-voltage diagram shown in Figure 2. At early on- and off-time, we observe significant EM induction effects. It is only at late off-times that we can identify typical over-voltage effects which are characteristic of the IP responses. The fact that EM dominates the data at early times and IP effects dominate the late-time data suggests it may be possible to separate the EM and IP responses in time.

For a clearer demonstration of this, we view only the off-time data, and plot them on a log-log plot as shown in Figure 4. Black, blue, and red lines correspondingly indicate observed, fundamental, and IP responses; solid and dotted lines distinguish negative and positive data. At early times, the fundamental response is much greater than the IP data; this is the region of EM dominance. At later times, the IP signal is much greater than the fundamental; this is the region of IP-dominance. Importantly, there is an intermediate time region when both EM and IP are considerable. Our following inversion workflow is based upon this natural separation of EM and IP in time.

3D TEM-IP INVERSION WORKFLOW

Our inversion workflow is based upon Kang and Oldenburg (2016) which was built for an inductive source case, but is applicable here. Figure 5 shows the 3D TEM-IP inversion workflow to be applied. The first step is to invert the TEM data to recover the 3D σ_∞ model. As in our inductive source work, we use only early time data that we feel are not IP-contaminated. We note that these early time data have previously been considered as "noise" in conventional analyses and hence have been thrown away. However, here we consider these as "signal" and use them to recover a better conductivity model. Another possibility for obtaining a background conductivity is to use the steady-state fields just prior to switching the current off. These are the potentials that are traditionally used in DC-IP inversion. Inversion of these data yields a conductivity that is $\sigma_0 = \sigma_\infty(1-\eta)$ but if η is small enough then this will be a reasonable approximation to σ_∞. The inversion of DC data is analogous to inverting only one frequency in a frequency-domain data set. Hence it might be expected that inverting data at multi-times (equivalent to multi-frequencies) would produce a better result. Our experience verifies this. Nevertheless, the DC fields are valuable and we wish to use them. The options are to invert the DC and TEM data together, or treat them as two separate data sets. For the present we have chosen the latter since we then do not have to contend with the issue that the DC fields are really σ_0. The approach implemented here is first to invert the DC data and then use the resulting model as a starting and reference model for the TEM inversion

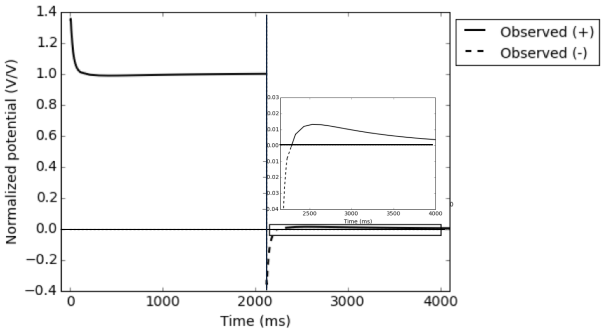

Figure 3. Observed voltage with EM induction effects. EM effects dominate the early off-time data.

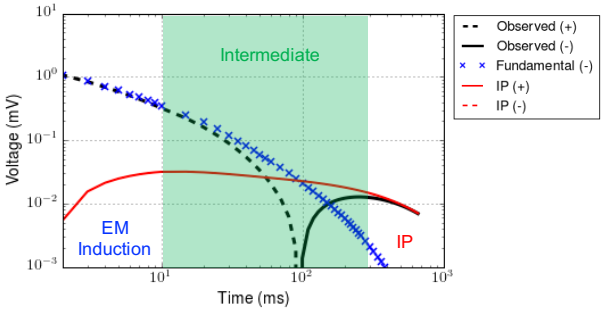

Figure 4. Transients of observed (black line), fundamental (blue crosses) and IP (red line) at the off-time in the log-log plot. Solid and dotted lines distinguish positive and negative datum.

The second step of the workflow is EM decoupling. The estimated conductivity model, σ_{est}, from step 1 is used to generate raw IP data according to

$$d^{IP}_{raw} = d^{obs} - F[\sigma_{est}], \quad (4)$$

where d^{obs} is the observed data, $F[\sigma_{est}]$ is estimated fundamental data. Here, we identify that the predicted fundamental response might be different from true fundamental response, because σ_{est} is not the same as σ_∞. Potential errors in raw IP data will be significant especially at early times, but they will decrease as time increases. The effective region for EM-decoupling will be in the intermediate time when both EM and IP are considerable (Figure 4). Note that at late time (IP-dominant) EM-decoupling may not be required.

The final step in the process is to carry out the IP inversion. We adopt the conventional IP inversion approach (e.g. Oldenburg and Li, 1994), which uses a linear form of IP responses written as

$$d^{IP}(t) = G\tilde{\eta}(t), \quad (5)$$

where G is the sensitivity function and $\tilde{\eta}(t)$ is the pseudo-chargeability. The conductivity model σ_{est} is required to generate the sensitivity matrix. We invert each time channel

of IP data separately, and recover pseudo-chargeability at multiple times. Interpreting this recovered pseudo-chargeability to extract intrinsic IP information such as η, τ, and c is possible, but we do not treat that in this study.

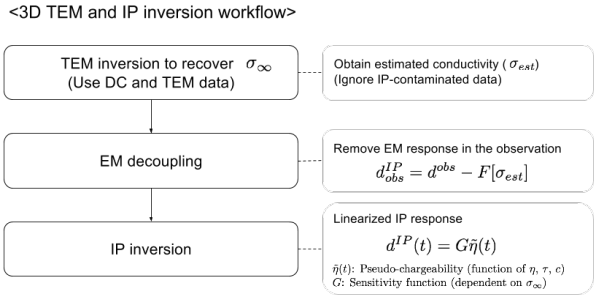

Figure 5. A 3D TEM-IP inversion workflow for galvanic source TEM data.

GALVANIC SOURCE EXAMPLE

Synthetic TEM data

As an example, we use a galvanic source and multiple receivers which measures voltages as shown in Figure 3. Four blocks (A1-A4) presented in Figure 6 have different σ_∞ and η values (see Table 1); all blocks have τ =0.5 sec and c=1 (Debye model). Only A2 and A3 blocks are chargeable. The length of the transmitter wire is 4.5 km and potential differences between two electrodes along easting lines are measured at 625 locations. The measured time channels are logarithmic-based ranging from 1-600 ms (60 channels). Computed responses at 5, 80, and 350 ms are shown in Figure 7. At 5 ms, EM induction effects are dominant, and all data are negative. At 80 ms, both EM and IP effects are considerable, but still all data are negative. Note that A2 and A3 are chargeable, but A1, which is conductive, is not. Therefore, it is difficult to differentiate chargeability and conductivity anomalies just by looking at observed data at 80 ms. At 350 ms, EM induction effects are significantly decayed, hence IP is dominant. Only A2 and A3 show positive anomalies that originate from chargeability. Depending on the measured time window, and IP parameters of chargeable bodies, we could have data in IP-dominant time or not. Hence, whenever our measured time window is not late enough to be considered as IP-dominant time, EM-decoupling is crucial step. Note that the A1 anomaly at 80 ms could be misinterpreted as a chargeable response, if this is the latest time channel.

Table 1. Conductivity at infinite frequency and intrinsic chargeability values for five units: A1-A4 and half-space.

Division	A1	A2	A3	A4	half-space
σ_∞ (S/m)	1	0.01	0.1	0.001	0.01
η (V/V)	0	0.1	0.1	0	0

3D DC and TEM inversion

To recover σ_∞, we use the first six channels of the TEM data (1-6 ms), which have minor contamination from IP. In addition, we have DC data which contain IP effects, but have minor EM induction effects. We first invert the DC data, and recover 3D conductivity. By using the recovered DC conductivity as a reference model, we invert the TEM data. The recovered conductivity models from the 3D DC and TEM inversions are shown in Figure 8. The conductive blocks A1 and A3 are much better imaged with the TEM inversion.

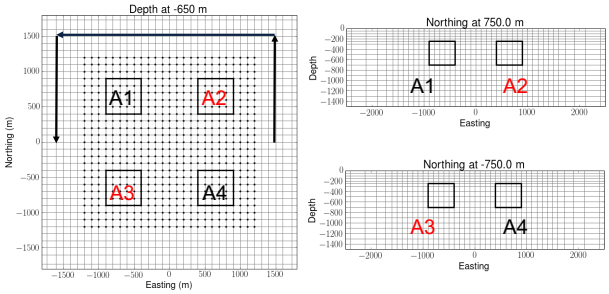

Figure 6. Plan and section views of the 3D mesh. Black solid lines show the boundaries of four blocks (A1-A4). Only A2 and A3 are chargeable. Arrows indicate a wire path for the galvanic source.

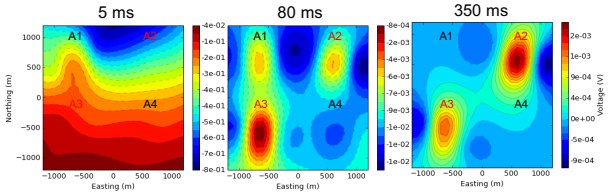

Figure 7. Plan maps of the observed TEM data at 5 ms (left panel), 80 ms (middle panel), 350 ms (right panel). Dashed and solid contours differentiate negative and positive data.

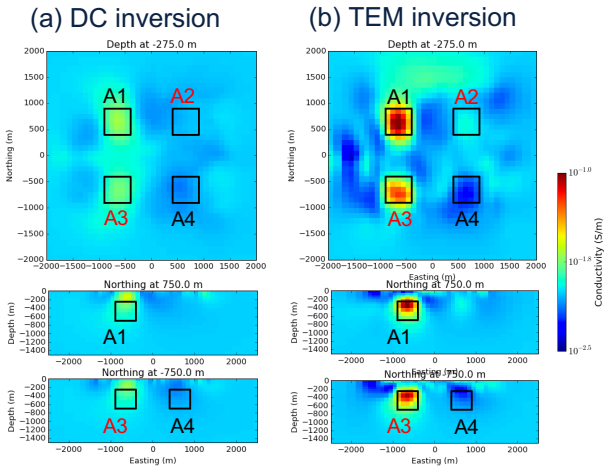

Figure 8. Recovered conductivity models from (a) DC and (b) TEM inversions.

EM-decoupling

The next step is EM-decoupling. We implement Eq. (4) using σ_{est} from the TEM inversion (Figure 8b). In Figure 9, we present observed, predicted and raw IP data at 80 ms. At this time, both EM and IP effects are considerable. Our EM-decoupling procedure effectively removes EM effects due to conductivity especially for regions close to A1 (not chargeable) and A3 (chargeable). Removing the conductive anomaly at A1 is crucial, because this could have been misinterpreted as chargeable anomaly.

The crucial aspect of our EM-decoupling procedure is the effect of the background conductivity. To show this we consider two other candidates, namely a) true σ_∞, b) half-space conductivity (σ_{half}). We compare performance of EM-decoupling for all three different conductivity models. Figure 10 shows predicted fundamental response and IP data

generated using the three conductivity models. The EM response computed using σ_∞ clearly shows two conductive anomalies. A similar conclusion can be drawn from the results using σ_{est}. The A1 and A3 conductive anomalies are effectively removed resulting in A1 being stronger anomaly than A3. As shown in the left panel Figure 7, A3 was stronger in the observation. The half-space conductivity however does a poor job at predicting the EM effects and the resultant raw IP data have numerous artifacts, especially at A1 and A3 where there are conductive blocks and where the IP data is overestimated. If these data are input to a 3D IP inversion, they produce strong artefacts from which incorrect conclusions can be drawn.

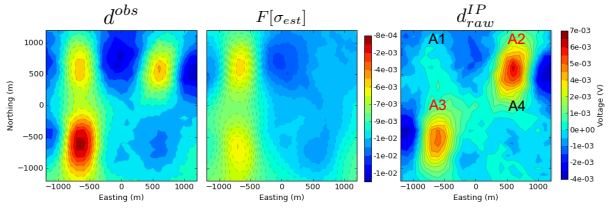

Figure 9. Plan maps of observed (left panel), estimated fundamental (middle panel) and raw IP (right panel) at the 80 ms.

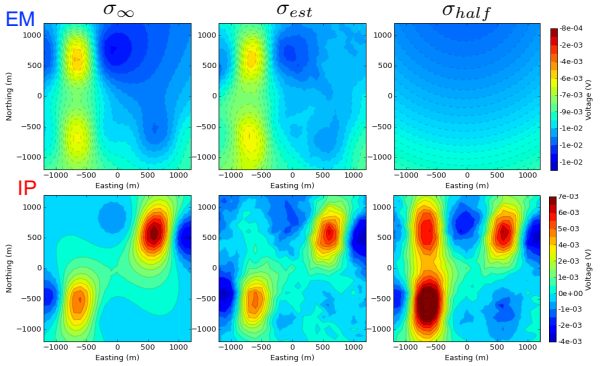

Figure 10. Comparison of EM (top panel) and IP (bottom panel) responses obtained from three different conductivity models. (a) true σ_∞, b) σ_{half}, and c) σ_{est} from TEM inversion.

3D IP inversion

To recover 3D pseudo-chargeability, we invert raw IP data sets at 80 ms obtained using the estimated conductivity, σ_{est}, from the TEM inversion. This conductivity is used to generate the linearized sensitivities as outlined in Kang and Oldenburg (2016). This linear system is inverted with the added constraint of positivity on the chargeability (Oldenburg and Li, 1994). Depth weighting, invoked for the airborne case, was not used for this 3D IP inversion. The recovered 3D pseudo-chargeability model is shown in Figure 11. The two true chargeable bodies, A2 and A3, are well imaged without significant artefacts. It is also noted that the pseudo-chargeability of A2 is stronger than that for A3. This is compatible with the known amplitude from the true IP data shown in Figure 10.

CONCLUSIONS

In this study, we have applied the 3D TEM-IP inversion workflow to a galvanic source TEM example. First, we inverted DC data and recovered a 3D conductivity. Then, by using that as a reference model, we inverted six of the earliest time channels of TEM data, which have minor IP-contamination, and recovered a 3D conductivity. These early TEM data often have been thrown away because they are considered as "noise". However, by considering them as "signal" and inverting them, we recovered a better conductivity model. Second, the recovered conductivity, σ_{est} was used in our EM-decoupling procedure to generate raw IP data. The procedure was effective for removing EM induction in the observations, especially for regions close A1 and A3, which had significant conductivity responses. Third, we inverted the IP data set generated from the TEM conductivity model using conventional 3D IP inversion. The recovered pseudo-chargeability successfully imaged two true chargeable anomalies A2 and A3. This demonstrates that our TEM-IP inversion workflow can be effective for recovering a good estimate of electrical conductivity, for removing EM signals from IP data, and for obtaining a 3D distribution of pseudo-chargeability.

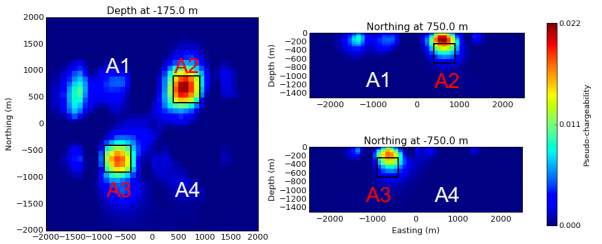

Figure 11. Plan and section views of the recovered pseudo-chargeability.

REFERENCES

Flis, M. F., G. A. Newman, and G. W. Hohmann, 1989, Inducedpolarization effects in timedomain electromagnetic measurements: Geophysics, 54, 514–523.

Kang, S., and D. W. Oldenburg, 2016, On recovering distributed IP information from inductive source time domain electromagnetic data (in revision): Geophysical Journal International.

Marchant, D., E. Haber, and D. Oldenburg, 2014, Three-dimensional modeling of IP effects in time-domain electromagnetic data: Geophysics, 79, E303–E314.

Oldenburg, D., and Y. Li, 1994, Inversion of induced polarization data: Geophysics, 59, 1327–1341.

Pelton, W., S. Ward, P. Hallof, W. Sill, and P. Nelson, 1978, Mineral discrimination and removal of inductive coupling with multifrequency IP: Geophysics, 43, 588–609.

Seigel, H., 1959, Matehmatical formulation and type curves for induced polarization: Geophysics, 24, 547–565.

Smith, R. S., P. Walker, B. Polzer, and G. F. West, 1988, The time-domain electromagnetic response of polarizable bodies: an approximate convolution algorithm: Geophysical Prospecting, 36, 772–785.

Weidelt, P., 1982, Response characteristics of coincident loop transient electromagnetic systems: 47, 1325–1330.

Wynn, J. C., and K. L. Zonge, 1975, EM coupling, its intrinsic value, its removal and the cultural coupling problem: Geophysics, 40, 831–85